

# Rock magnetic and geochemical analyses of surface sediment characteristics in deep ocean environments: A case study across the Ryukyu Trench

Noriko Kawamura<sup>1\*</sup>, Kiichiro Kawamura<sup>2</sup>, and Naoto Ishikawa<sup>1</sup>

<sup>1</sup>Graduate School of Human and Environmental Studies, Kyoto University, Yoshida-nihonmatsu-cho, Kyoto 606-8501, Japan

<sup>2</sup>Fukada Geological Institute, 2-13-12, Honkomagome, Bunkyo, Tokyo 113-0021, Japan

(Received September 30, 2006; Revised November 29, 2007; Accepted November 30, 2007; Online published March 3, 2008)

Magnetic minerals in marine sediments are often dissolved or formed with burial depth, thereby masking the primary natural remanent magnetization and paleoclimate signals. In order to clarify the present sedimentary environment and the progressive changes with burial depth in the magnetic properties, we studied seven cores collected from the Ryukyu Trench, southwest Japan. Magnetic properties, organic geochemistry, and interstitial water chemistry of seven cores are described. Bottom water conditions at the landward slope, trench floor, and seaward slope are relatively suboxic, anoxic, and oxic, respectively. The grain size of the sediments become gradually finer with the distance from Okinawa Island and finer with increasing water depth. The magnetic carriers in the sediments are predominantly magnetite and maghemized magnetite, with minor amounts of hematite. In the topmost sediments from the landward slope, magnetic minerals are diluted by terrigenous materials and microfossils. The downcore variations in magnetic properties and geochemical data provided evidence for the dissolution of fine-grained magnetite with burial depth under an anoxic condition.

**Key words:** Marine sediments, rock magnetic properties, early diagenesis, interstitial water, sedimentary environments.

## 1. Introduction

Rock magnetic properties of marine sediments change with variations in the abundance, type, and grain size of magnetic minerals. Magnetic iron oxides, such as magnetite ( $\text{Fe}_3\text{O}_4$ ), maghemite ( $\gamma\text{Fe}_2\text{O}_3$ ), hematite ( $\alpha\text{Fe}_2\text{O}_3$ ), titanomagnetite ( $\text{Fe}_3\text{O}_4\text{-Fe}_2\text{TiO}_4$ ), and titanohematite ( $\text{Fe}_3\text{O}_4\text{-Fe}_2\text{TiO}_3$ ), are common magnetic minerals in marine sediments. These magnetic minerals are supplied as grains of detrital or biogenic origin. Consequently, magnetic properties have been used as proxies of detritus-supply changes for recording paleoenvironmental and paleoclimate changes (e.g., Stoner *et al.*, 1995; Kissel *et al.*, 1998; Walden *et al.*, 1999; Evans and Heller, 2003).

In general, organic matter in sediments undergoes decomposition by bacterial activity during burial, which changes the oxidation-reduction conditions in the sediments. Bacterial decomposition of organic matter is an example of early diagenesis. During the early diagenetic regime, iron oxides are dissolved, causing changes in the grain size distribution of magnetic minerals (e.g., Karlin and Levi, 1983; Torii, 1997; Yamazaki *et al.*, 2003). Ferromagnetic iron sulfides are also crystallized under anoxic conditions as early diagenesis proceeds (e.g., Leslie *et al.*, 1990a, b; Robinson *et al.*, 2000; Liu *et al.*, 2004; Garming *et al.*, 2005). The diagenetic changes and authigenic for-

mation of magnetic minerals alter the magnetic properties of the sediments. As a result, the original magnetic information for paleoenvironmental and paleoclimate conditions are masked by the early diagenetic effects. It is thus essential to clarify the original magnetic mineral assemblage from the alteration products in the marine sediments.

Early diagenetic effects on magnetic properties are controlled by various chemical factors during the sedimentation and post-depositional processes, such as, for example, the supply rate of organic matter, temperature, and diffusion of oxygen from oxic bottom water into the sediments (e.g., Froelich *et al.*, 1979; Berner, 1980; Carman and Rahm, 1997; Rey *et al.*, 2005). Such factors are also expected to affect magnetic mineral composition in marine sediments. Many previous studies of diagenetic effects on magnetic properties have been reported from continental shelf sites and from enclosed basins (e.g., Leslie *et al.*, 1990a, b; Robinson *et al.*, 2000; Liu *et al.*, 2004; Garming *et al.*, 2005). Kawamura *et al.* (2007) suggested that the dissolution of magnetic minerals in hemipelagic sediments from the southern Okhotsk Sea was significantly accelerated due to the high supply of organic matter. However, there are few studies of diagenetic effects on open marine sediments. The relationship between factors controlling early diagenesis and magnetic properties of marine sediments has not been fully understood.

The Ryukyu Trench is located on the eastern side of the Ryukyu Island Arc along the western margin of the subtropical North Pacific (Fig. 1). The temperature of the seawater in the Ryukyu Trench rapidly decreases from 0 to 1000 m, being stable below 1000 m. The density increases with wa-

\*Now at Geological Survey of Japan, AIST, 1-1-1 Higashi, Tsukuba 305-8567, Japan.

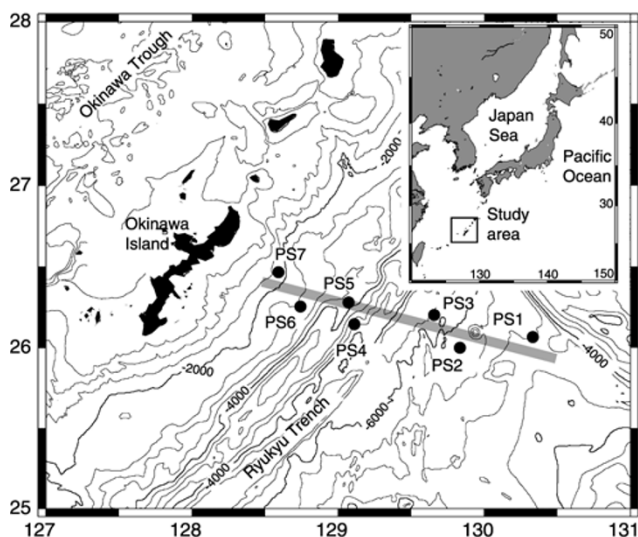


Fig. 1. Map showing the location of coring sites. The gray line shows the core transect.

ter depth (Hase and Minato, 2003). Sedimentary environments are expected to change with water depth across the Ryukyu Trench.

We investigated sedimentary environments in the Ryukyu Trench, based on rock magnetic properties and the organic geochemistry of the surface sediments within approximately 30 cm of the sediment-water interface and the geochemistry of interstitial and overlying bottom waters. The aim of this study was to distinguish between the original magnetic mineral assemblage and subsequent overprints and to clarify the diagenetic factors affecting magnetic properties of the hemipelagic sediments.

## 2. Samples

Sediment cores up to 33 cm in length were collected using a multiple corer at seven sites across the Ryukyu Trench during the R/V *Hakuohmaru* cruise KH05-1 in 2005 (Table 1, Fig. 1). The multiple corer can recover undisturbed surface sediments with bottom water. The coring sites PS4, PS5, PS6, and PS7 are located on the landward slope in the Ryukyu Trench, site PS3 on the trench floor, and sites PS1 and PS2 on the seaward slope (Figs. 1 and 5; Table 1). These coring sites were chosen from the transect perpendicular to the trench, with progressively increasing water depth as one moves seaward from Okinawa Island to the trench floor, and decreasing water depth from the trench floor to the seaward slope.

Cores PS6 and PS7 from water depths shallower than approximately 3,000 m are composed of sandy clay with foraminifera (Fig. 2). The sediment color of core PS6 is yellow brown, and in core PS7, the color changes downward from oxidized dark grayish-yellow (0–21 cm) to grayish-olive (21–29 cm). Cores PS4 and PS5 are composed of non-foraminiferous clayey silt, and the colors are oxidized olive brown and dark grayish yellow, respectively. The carbonate compensation depth is inferred to exist between 3,000 m and 3,800 m in this area. Core PS3 from the trench floor and cores PS1 and PS2 from the seaward slope are characterized by dark olive brown to olive brown silty clay. Ac-

Table 1. Positions and water depths of coring sites.

Core ID	Latitude (N)	Longitude (E)	Water depth (m)
PS1	26° 04.00	130° 20.00	4910
PS2	25° 59.96	129° 50.02	5710
PS3	26° 12.22	129° 39.38	6336
PS4	26° 08.79	129° 06.62	5334
PS5	26° 17.67	129° 06.86	3849
PS6	26° 05.98	128° 42.98	3027
PS7	26° 20.05	128° 30.02	1964
RN95-PC4	26° 09.40	128° 40.90	2787

cording to our core observation, the grain sizes of the sediments become gradually finer with increasing distance from the Okinawa Island, and finer with increasing water depth.

A volcanic ash layer was observed at 28–32 cm below the seafloor (cmbsf) in core PS3. Based on refractive index values of the volcanic glass fragments from this layer, which range from 1.510 to 1.514, Kawamura and Kawamura (2006) correlated this ash layer with the K-Ah tephra, a widespread tephra that was erupted at about 7300 yr B.P. (Machida and Arai, 2003). Using this horizon, the sedimentation rate at site PS3 was estimated to be approximately 4 cm/kyr. This agrees with the results of Ujiie and Ujiie (1999) on core RN95-PC4, which is located near the site PS6. Based on Accelerator Mass Spectrometer (AMS)  $^{14}\text{C}$  ages for *G. sacculifer* larger than 149  $\mu\text{m}$ , these researchers suggested that the sedimentation rate for core RN95-PC4 is 3 cm/kyr. According to the above estimation of sedimentation rates, the sediments in this study were deposited during the Holocene. Kawamura and Ishikawa (2006) reported that the 20 mT demagnetized remanent magnetization of u-channel samples from near-shore cores revealed the lack of secular variations. Therefore, magnetostratigraphy was not used for age estimation.

## 3. Methods

### 3.1 Rock magnetic analyses

Samples for magnetic measurements were taken with 7-cc plastic cubes at 2.2-cm intervals for rock magnetic analyses. Measurements of magnetic susceptibility ( $\chi$ ), anhysteretic remanent magnetization (ARM), and isothermal remanent magnetization (IRM) were performed on the cube samples while the sediments were wet. The  $\chi$  values were measured using a KLY-3S magnetic susceptibility meter (AGICO Inc.). The ARM was induced on each sample with a DC biasing field of 0.1 mT in a peak alternating field of 100 mT. The IRMs were imparted at 2.5 T and at a back-field of 0.3 T with a MMPM-9 pulse magnetizer (Magnetic Measurements Ltd.). The IRM at 2.5 T is regarded as the saturation IRM (SIRM) in this paper. The ARM and IRM were measured with a 2G-Enterprises 760R superconducting rock magnetometer. After the above measurements were conducted, the samples were dried at 60°C in an electric oven and weighed to calculate dry-based mass-specific magnetic parameters. The  $\chi_{\text{ARM}}$  value was calculated by dividing the ARM intensity with the strength of the DC biasing field (0.1 mT). The S ratio ( $S_{-0.3\text{T}}$ ) was calculated

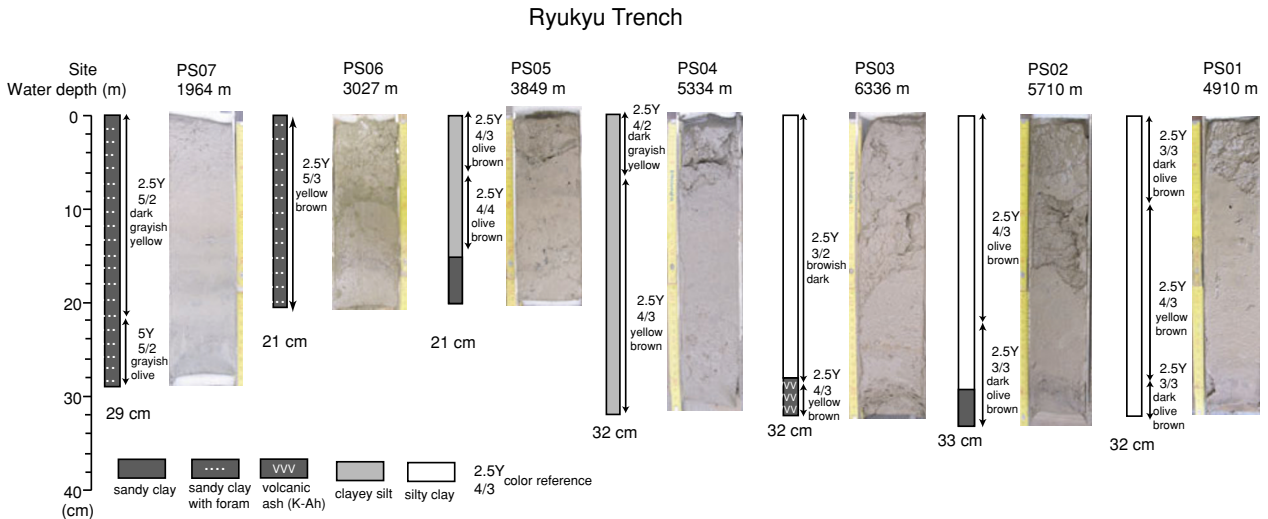


Fig. 2. Lithologies, core photographs and total lengths of the core samples from the Ryukyu Trench.

after the definition of Bloemendal *et al.* (1992):

$$S_{-0.3T} = [1 - (IRM_{-0.3T}/SIRM)]/2$$

In order to identify the magnetic minerals, thermomagnetic analyses and thermal demagnetization of composite IRMs were performed on selected samples. Low-temperature magnetometry was performed using a Quantum Design magnetic property measurement system (MPMS-XL5). Approximately 50 mg of dry sediments was wrapped inside plastic film. First, an SIRM was imparted to the sample at 6 K in a field of 3 T, and then the magnetization changes with temperature were measured during the warming cycle from 6 K to 300 K in a zero field. Next, the samples were cooled from 300 K to 6 K in the presence of a field of 3 T, and then the magnetization changes were measured in a zero field during warming back to 300 K. Thermal demagnetization of composite IRMs was performed on several samples following the method of Lowrie (1990) and Ishikawa and Frost (2002). The sediments (approx. 50 mg) were packed in a small quartz cup (5 mm in diameter and 10 mm in height). A magnetic field of 2 T was applied along the vertical direction of the cup, and then a field of 0.12 T was applied perpendicular to the axis using the pulse magnetizer. The IRM was measured with the 2G-760R magnetometer.

Measurements of hysteresis loops (HL) and direct-current demagnetization (DCD) of SIRM (*M<sub>rs</sub>*) required for the determination of the coercivity of remanence (*H<sub>cr</sub>*) were performed on samples 10–30 mg from selected horizons with an alternating gradient magnetometer (AGM, Model 2900-02, Princeton Measurements Corporation). The maximum applied field was 1.0 T, and the field increment was 2 mT during the HL and DCD measurements. The coercivity (*H<sub>c</sub>*), *M<sub>rs</sub>*, saturation magnetization (*M<sub>r</sub>*), and high-field magnetic susceptibility (HFMS) were determined after the correction for the high-field slope of the HL between 0.7 T and 1.0 T. Ferromagnetic susceptibility ( $\chi$ ) was calculated as the difference between  $\chi$  and HFMS.

### 3.2 Organic geochemistry

Concentrations of total carbon (TC), total organic carbon (TOC), and total nitrogen (TN) at the topmost horizons of the seven cores were analyzed using a CHN (carbon, hydrogen, and nitrogen) analyzer (2400 Series II, Perkin-Elmer Inc.). For the TOC analysis, approximately 20 mg of dried sediments was reacted with 1N HCl. The TOC/TN ratios represent the sources of organic materials in the sediments, and high values indicate that the sediments are rich in organic materials of detrital origin (e.g., Emerson and Hedges, 1988).

### 3.3 Grain-size analysis

Samples for grain-size analyses were taken from the topmost part of the core samples. A wet sample of approximately 0.1 g was dispersed into boiling water in a glass beaker and then left for 24 h. The samples were further dispersed with an ultrasonic vibrator for 30–60 s just before the measurement. These samples were measured with a CIRAS 1064 laser diffraction particle analyzer. In this apparatus, water with sedimentary grains passes through a quartz slit (approx. 500  $\mu$ m in width) where they are constantly shot with a laser. The laser is dispersed according to particle size.

### 3.4 Interstitial water geochemistry

The Eh, pH, and the dissolved oxygen (DO) of interstitial water were directly measured with a DO meter (HORIBA, Ltd., OM-51-2). The measurement procedures followed those of Passier *et al.* (1998). The recovered cores were cut and capped immediately on board after the core recovery during 1 day. The geochemical data were obtained in the water just above the sediments (bottom water) and on the surface of the split cores. The measurement was carried out at each of the following three zones with different color—the brownish oxidized zone, the yellowish transition zone, and the reductive olive zone—in descending order.

## 4. Results

### 4.1 Thermomagnetic analyses

Low-temperature magnetometry and demagnetization of composite IRMs were performed on samples at 1 cmbsf

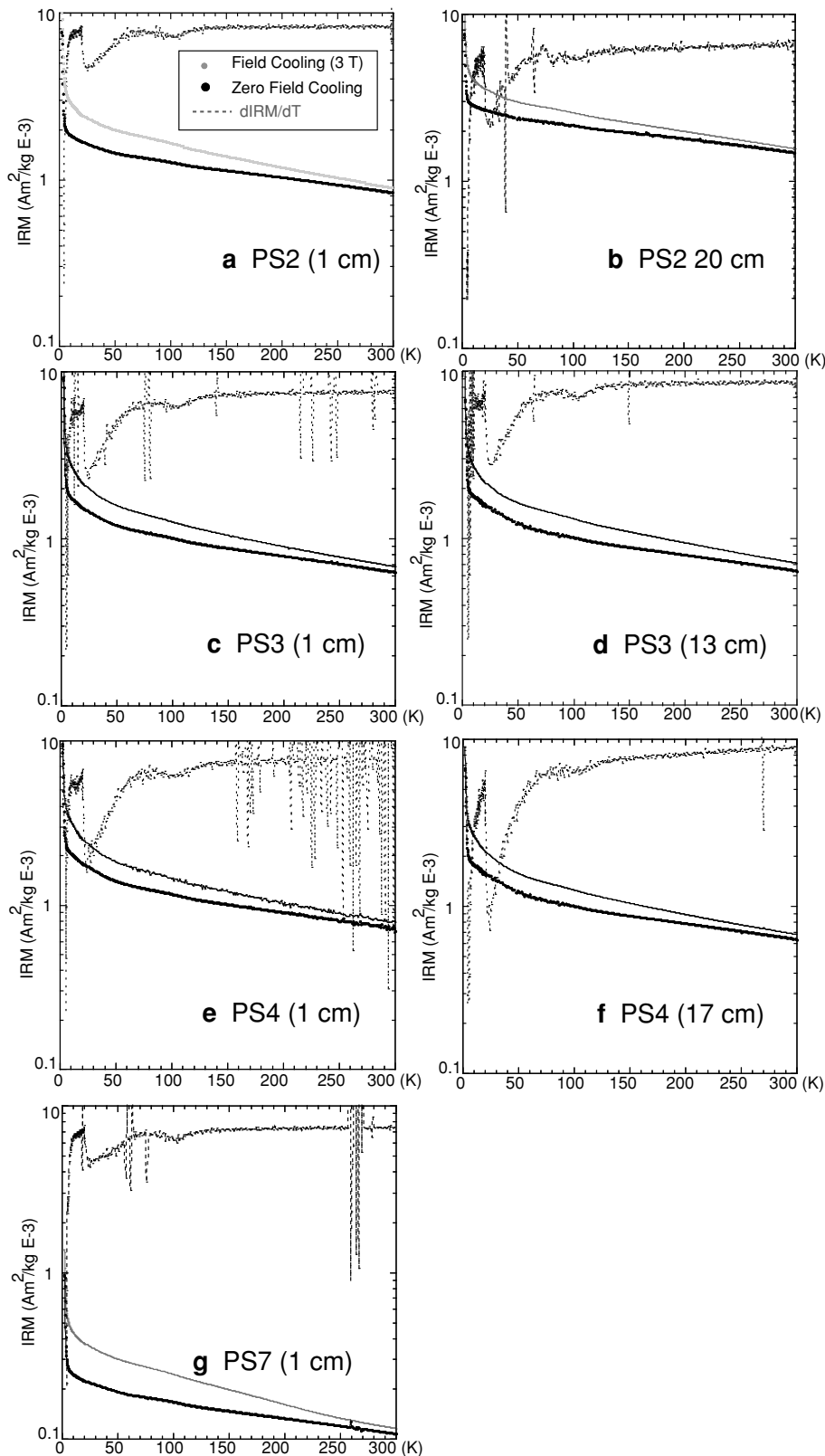


Fig. 3. Thermal demagnetization curves of the low-temperature SIRM imparted after zero-field cooled (ZFC, small gray circle) and field cooled (FC, black circle). Decay curves of IRM from 6 K to 300 K are presented together with their derivatives (dIRM/dT, dashed line).

and 20 cmbsf for core PS2, at 1 cmbsf and 13 cmbsf for core PS3, at 1 cmbsf and 17 cmbsf for core PS4, and at 1 cmbsf for core PS7 (Fig. 3). A slight decrease in IRM at about 100 K was suggested for all samples based on the changes in the derivative of the IRM curves, although this

decrease is subtle. This change is interpreted to be the Verwey transition of magnetite, and its suppression is indicative of oxidation (maghematization) of magnetite (Verwey, 1939; Özdemir *et al.*, 1993; Torii, 1997). Results of thermal demagnetization of composite IRMs from the samples

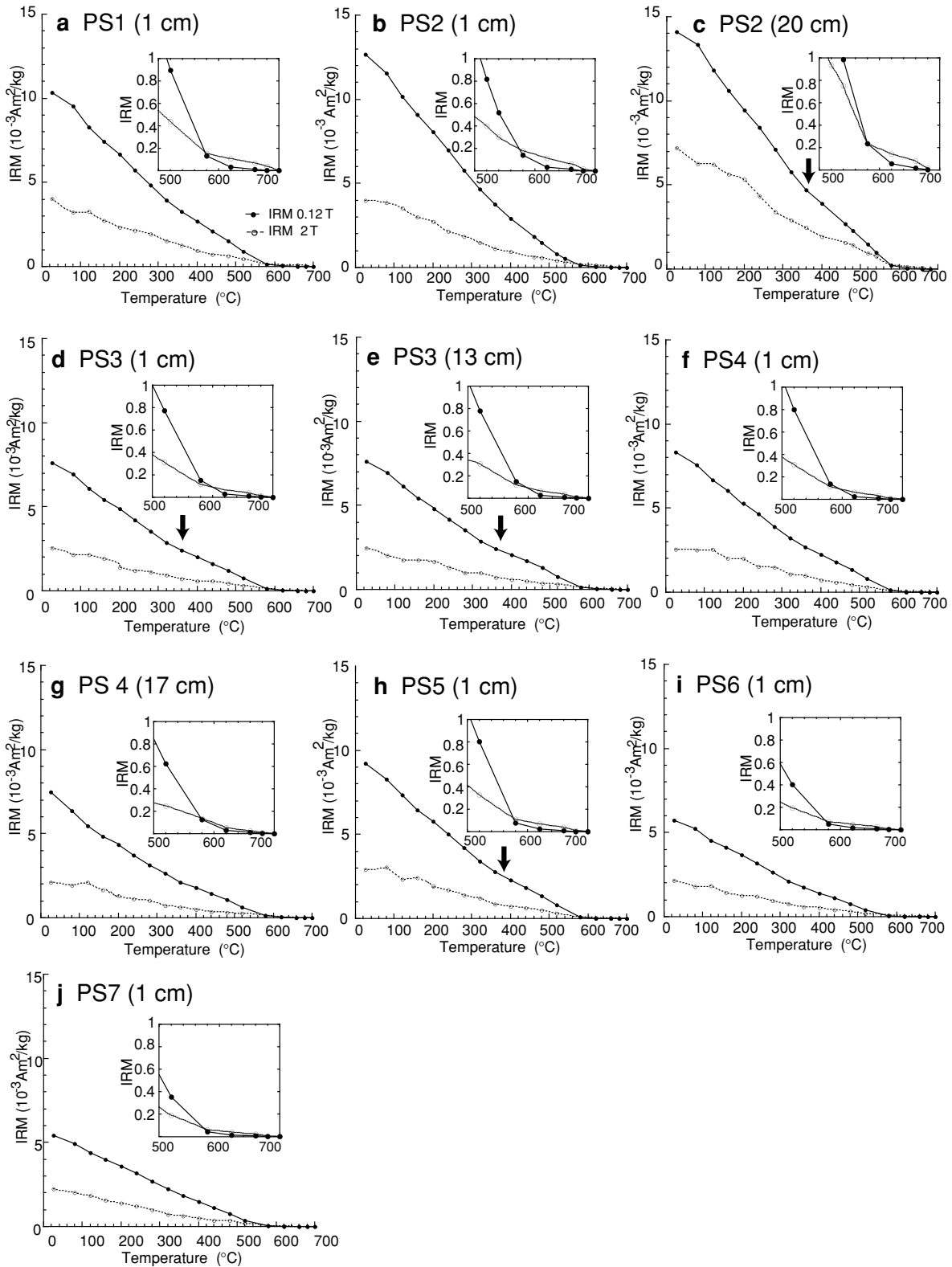


Fig. 4. Results of thermal demagnetization of composite IRMs for samples from 1 cmbsf and 20 cmbsf of core PS2. Arrows show inflection possibly caused by maghemite decomposition.

are shown in Fig. 4. The soft ( $<0.12$  T) and hard (0.12–2 T) components of IRMs were completely demagnetized at  $580^{\circ}\text{C}$  and  $680^{\circ}\text{C}$ , respectively, indicating the presence of magnetite and hematite. A slight inflection of the demagnetization curve of the IRM components at  $300\text{--}400^{\circ}\text{C}$  might indicate decomposition of maghemite during heating (e.g.,

Ishikawa and Frost, 2002). These thermomagnetic results suggest that the principal magnetic minerals are magnetite, maghemitized magnetite, and hematite.

#### 4.2 Characterization of the core-top sediments

The grain size distributions of the topmost sediments ( $0\text{--}2.2$  cmbsf) are shown in Fig. 5. In cores PS1 and PS2,

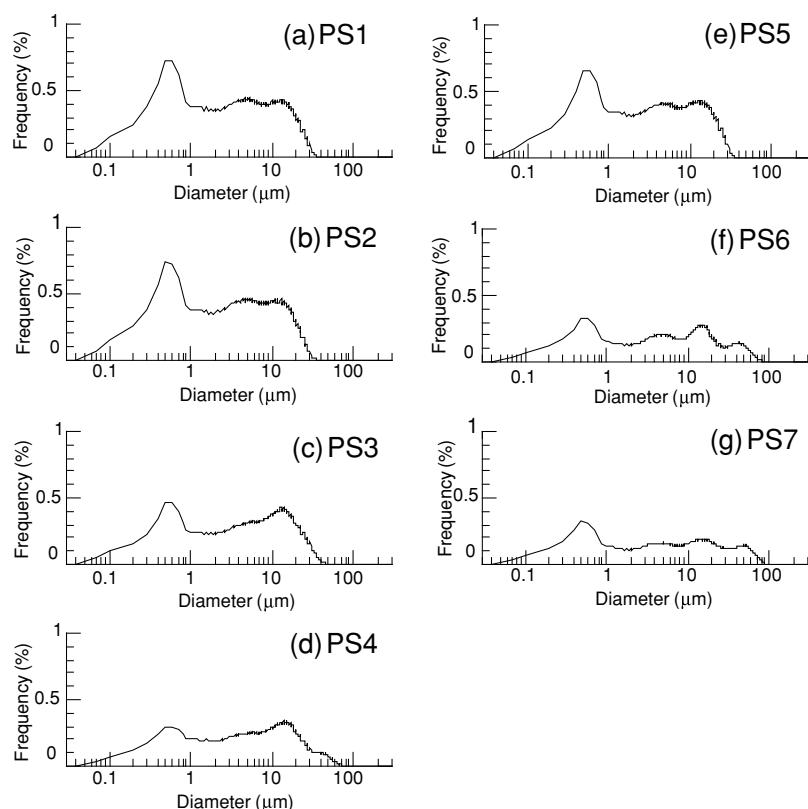


Fig. 5. Grain-size distributions of the topmost sediments of all cores.

there is a plateau from 3 to 11  $\mu\text{m}$ . In cores PS3, PS4, and PS6, there is a small peak at approximately 10–11  $\mu\text{m}$ . Cores PS5, PS6, and PS7 have several broad bumps in the spectrum. Cores PS6 and PS7 show a broad distribution characterized by grains coarser than 40  $\mu\text{m}$ . These results are consistent with lithological data from cores PS6 and PS7 (Fig. 2).

The TC, TOC, and TOC/TN values of the topmost sediments are shown in Figs. 6(b, c, d), respectively. The TC shows relatively high values at sites PS6 (5.07 wt%) and PS7 (5.22 wt%) in the upper part of the landward slope where the sediments contain large amounts of foraminifera (Fig. 2). The TOC values range from 0.38 wt% to 0.49 wt%, and no significant difference was observed among the cores. Relatively high values of TOC/TN ratios (6.45–6.20) were observed at sites PS6 and PS7.

Bottom-water geochemistry data are shown in Fig. 6(e). The DO values were below 4 mg/l at sites PS3 and PS4, suggesting a relatively anoxic condition in the landward trench floor. A comparison between the cores indicates that the interstitial water conditions at the landward slope, trench floor, and seaward slope are relatively suboxic, anoxic, and oxic, respectively.

The  $\chi$ ,  $\chi_{\text{ARM}}$ , SIRM,  $S_{-0.3\text{T}}$ ,  $\chi_{\text{ARM}}/\chi$ , and SIRM/ $\chi$  values are shown in Figs. 6(f) to 6(k). The indicators of magnetic mineral concentration,  $\chi$ ,  $\chi_{\text{ARM}}$ , and SIRM, showed relatively lower values at sites PS6 and PS7 on the landward slope than those at sites PS1, PS2, PS4, and PS5 (Figs. 6(f, g, h)). Small drops in these values were observed at site PS3. It is inferred that the amount of magnetic minerals are lower at sites PS6 and PS7. The mineral diagnostic

parameter,  $S_{-0.3\text{T}}$ , displays high values above 0.95 at all sites. However, slightly lower values were observed at sites PS5, PS6, and PS7 on the landward slope. The magnetic grain-size indicator,  $\chi_{\text{ARM}}/\chi$  ratios, proposed by King *et al.* (1982), showed a high value at site PS7 and also a decreasing trend from the landward slope to the trench floor (Fig. 6(j)). A difference was also observed in SIRM/ $\chi$  between the landward-slope cores, the trench-floor, and the seaward cores (Fig. 6(k)). The SIRM/ $\chi$  ratios were high at the landward slope cores. The values of  $H_{\text{cr}}$  and  $H_{\text{c}}$  are shown in Fig. 6(l). The  $H_{\text{c}}$  values were stable, while the  $H_{\text{cr}}$  showed a slight increase on the landward slope. The  $\chi_{\text{f}}/M_{\text{s}}$  ratios at sites PS6 and PS7 are relative lower than those of the other sites (Fig. 6(m)).

The hysteresis parameters in cores PS1, PS3, and PS7 are shown in Fig. 7. The HL and DCD measurements were performed on three samples from the top horizon of each core. The HFMS values were below 1/10 of the  $\chi$  values of the samples, implying that contribution of paramagnetic minerals to  $\chi$  is not significant. The data for core PS7 showed slightly higher coercivity of remanence.

The  $M_{\text{rs}}/M_{\text{s}}$  and the  $H_{\text{cr}}/H_{\text{c}}$  ratios of the topmost sediments plotted in the pseudo-single domain (PSD) region of the Day plot (Day *et al.*, 1977) (Fig. 8), in which SD-MD and SD-SP mixing lines are shown according to Dunlop (2002). The data for cores PS6 and PS7 plot to the lower right of the data from the other cores.

#### 4.3 Downcore variations

We selected three cores for the analysis of downcore magnetic mineral and geochemical variations: PS2 (the seaward slope), PS3 (the trench floor), and PS4 (the land-

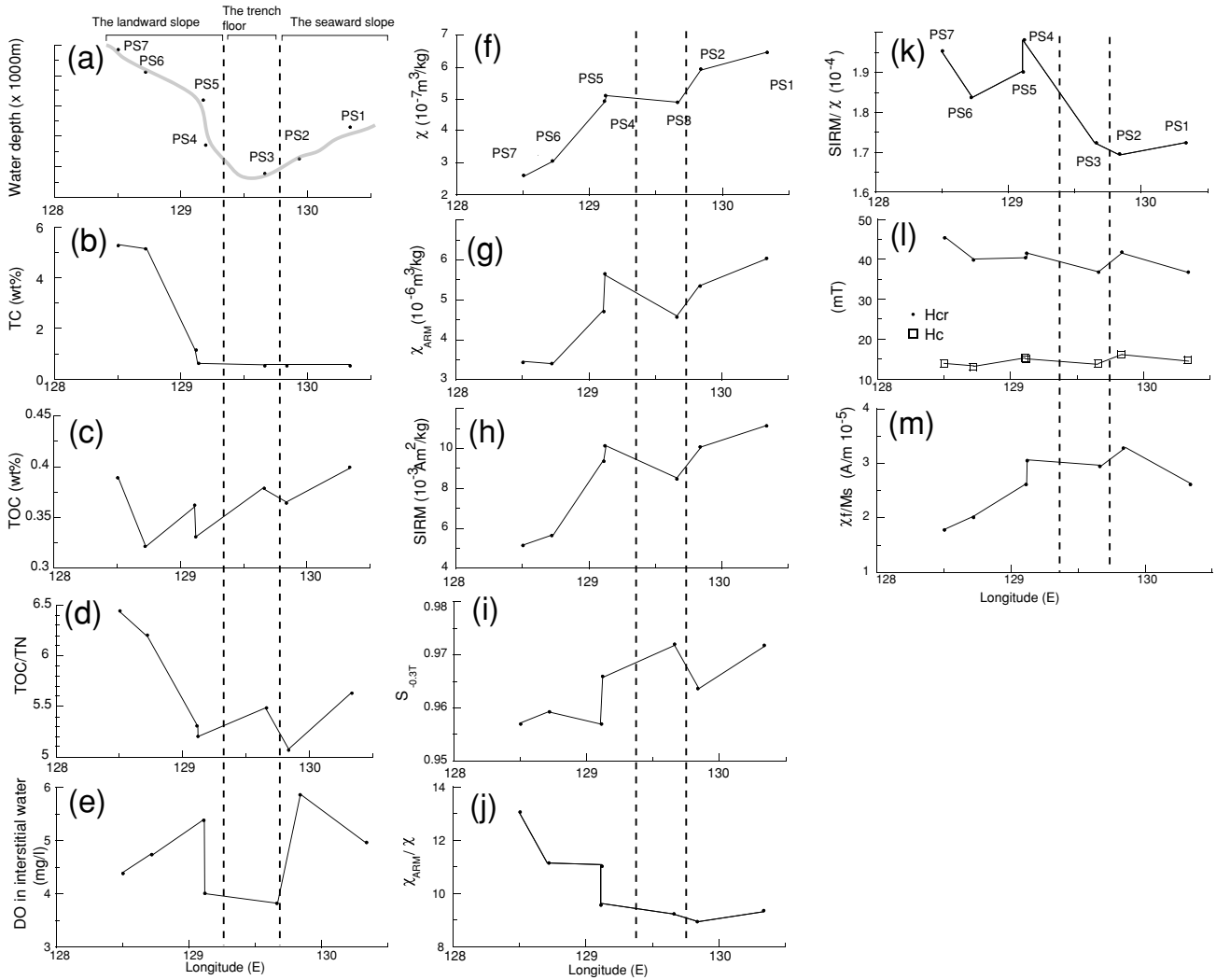


Fig. 6. Lateral variations of (a) water depth of the coring sites, (b) total carbon (TC), (c) total organic carbon (TOC), (d) TOC/TN, (e) dissolved oxygen (DO), (f)  $\chi$ , (g)  $\chi_{ARM}$ , (h) SIRM, (i)  $S_{-0.3T}$ , (j)  $\chi_{ARM}/\chi$ , (k) SIRM/ $\chi$ , (l) coercivity of remanence ( $H_{cr}$ ) and coercivity ( $H_c$ ), and (m)  $\chi_f$ /saturation magnetization ( $M_s$ ) of the topmost sediments.  $\chi_f$  shows ferromagnetic susceptibility, which was calculated as the difference between  $\chi$  and high field magnetic susceptibility (HFMS).

ward slope). These cores are composed of homogeneous silty clay except for the volcanic ash in core PS3 below 28 cmbsf. The grain size distribution in all three cores is similar (Kawamura and Kawamura, 2006), and the cores are suitable for discussing the changes of magnetic minerals.

Results from the pH, DO, and Eh at sites PS2, PS3, and PS4 are shown in Fig. 9(a, b, c). The pH value in core PS2 shows a constant and gradual decrease from 7.6 to 7.2 with depth, while the values in cores PS3 and PS4 first decrease in the topmost sediments and then switch to a gradual increasing trend. In contrast to the pH, the Eh gradually increases in core PS2, while the values in cores PS3 and PS4 first increase in the topmost sediments and then switch to a gradual decreasing trend. The DO decreases with burial depth at all coring sites.

The samples for rock magnetic experiments were taken from homogeneous horizons in the cores based on detailed observation of the cores. The lower part of core PS3, below 15 cmbsf, was not used for the measurements of hysteresis parameters because the lower part contains volcanic mate-

rials mixed in by bioturbation. In cores PS2 and PS3, the values of  $\chi$ ,  $\chi_{ARM}$ , and SIRM slightly increase downward. In core PS4, the values of  $\chi$  and  $\chi_{ARM}$  remain constant above 15 cmbsf, and a slight increase in  $\chi$  and decrease in  $\chi_{ARM}$  are observed below 15 cmbsf. The SIRM values gradually increases with depth in cores PS2 and PS3, and then remained nearly constant throughout the length of the PS4 core. The  $\chi_{ARM}/\chi$  ratios are stable in cores PS2 and PS3, while the ratio decreased below 15 cmbsf in core PS4. These changes in rock magnetic parameters occur in a very narrow range. The differences are small and observed only in the deepest two samples of each core, suggesting they might not be significant.

The values of  $H_c$  and  $H_{cr}$  display a small peak at 11 cmbsf and a slightly increasing trend with depth in core PS2. On the Day plot, the data points cluster with the exception of the peak of  $H_c$  at 11 cmbsf in core PS2. In core PS3,  $H_{cr}$  and  $H_c$  decrease with depth and display small drops at 5 cmbsf at the same horizon as the Eh peak. These values also gradually decrease downward in core PS4. On the Day plot for cores PS3 and PS4, the data does not cluster

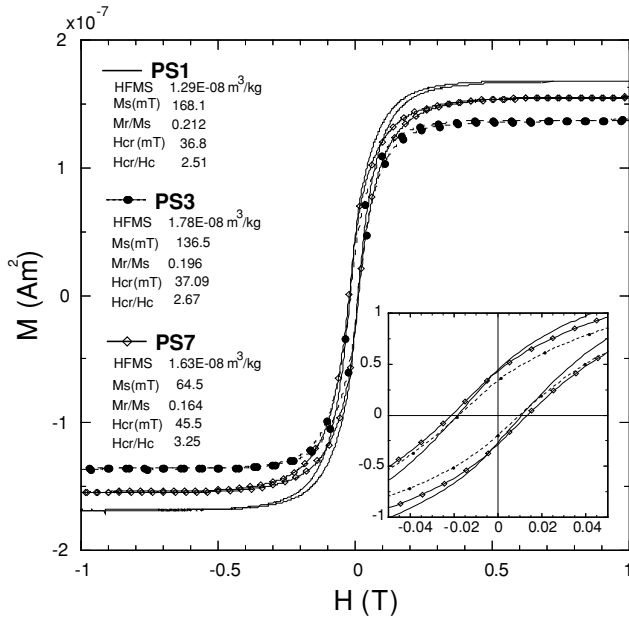


Fig. 7. Magnetic hysteresis curves of the topmost sediments from cores PS1, PS3, and PS7.

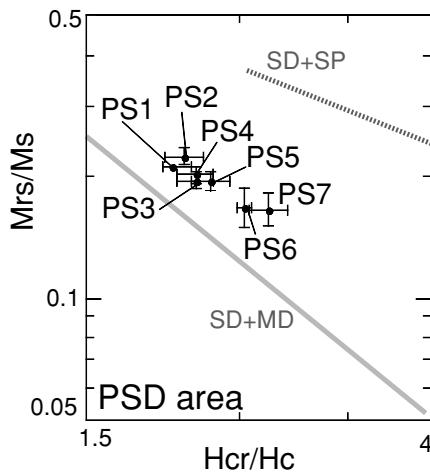


Fig. 8. Hysteresis ratios for the samples from the topmost sediments plotted on the Day plot (Day *et al.*, 1977). SD, PSD, and MD indicate single-domain, pseudo-single-domain, and multi domain fields of Day *et al.* (1977), respectively. The two lines show SD-SP and SD-MD mixing trends of Dunlop (2002).

well. In cores PS3 and PS4, the data show a trend towards the lower right with depth, corresponding to the changes in  $H_c$  and  $H_{cr}$ .

## 5. Discussion

### 5.1 Lateral distributions of sedimentary grains

The TOC/TN ratios of the samples range from 5.07 to 6.44. These values imply that organic matter in the sediments is of marine origin (Emerson and Hedges, 1988). High values of TC at sites PS6 and PS7, which consist of foraminifera-rich sediments, indicate that calcium carbonate is the main contributor to the TC.

Results of the thermo-magnetic measurements indicate that the magnetic minerals in the sediments are dominated by magnetite, maghemized magnetite, and hematite. The

low temperature FC-ZFC curves are separated from 6 to 300 K, which is consistent with but not diagnostic of the presence of high coercivity minerals (e.g., Hirt *et al.*, 2002; Liu *et al.*, 2006). We see no evidence of magnetosome chains in the FC-ZFC data (Moskowitz *et al.*, 1993). The magnetic minerals in the topmost sediments are believed to be primary terrigenous. The magnetization and magnetic susceptibility of hematite are two orders of magnitude smaller than those of magnetite and maghemite (Dunlop and Özdemir, 1997). Therefore, the variations in rock magnetic parameters of the topmost sediments can be satisfactorily explained by the variations in magnetite and maghemized magnetite concentrations in the sediments.

The variations in the concentration-dependent rock magnetic parameters,  $\chi$ ,  $\chi_{ARM}$ , and SIRM, indicate that magnetic minerals are more abundant at the coring sites on the seaward slope than the landward slope sites (Fig. 6). According to the lithology, the sediments from cores PS6 and PS7 consist of sandy clay with foraminifera, and the size of foraminifera is 50–500  $\mu\text{m}$  larger than magnetic minerals estimated on the Day plot (Figs. 2 and 5). This implies that the magnetite concentration in the landward slope sediments is diluted by the supply of terrigenous sediments and calcareous microfossils.

According to the lithologies and the grain-size distributions, the topmost sediments in cores PS6 and PS7 are relatively coarse (Figs. 2 and 5). The Day plot indicates that cores PS6 and PS7 contain coarser magnetic particles than the other cores in this transect (Fig. 8). However, the parameters  $\chi_{ARM}/\chi$  and  $SIRM/\chi$  suggest finer-grained magnetic particles in cores PS6 and PS7 (Fig. 6(j) and 6(k)). The reasons for the contradiction in these parameters are as follows. In Fig. 6(i), slightly lower  $S_{-0.3T}$  values are observed in cores PS5, PS6, and PS7, suggesting a larger proportion of high coercivity minerals. The results of high-temperature magnetometry indicate that hematite is present in all samples (Fig. 4). Hematite is one of high coercivity minerals (e.g., Dunlop and Özdemir, 1997). A sample with a higher hematite-to-magnetite ratio tends to show higher  $SIRM/\chi$  (Thompson and Oldfield, 1986). High  $SIRM/\chi$  in cores PS5, PS6, and PS7 may be due to relatively larger quantity of hematite at these sites. In Fig. 6(m), the  $\chi_f/M_s$  ratio of the topmost sediments show slightly lower values in cores PS6 and PS7, suggesting a lower abundance of superparamagnetic particles (Banerjee *et al.*, 1993). If the grain size of magnetite is larger than 0.05  $\mu\text{m}$  (stable SD size), we can expect that  $\chi_{ARM}$  is relatively high, and  $\chi$  is relatively low (Maher, 1988). Yamazaki and Ioka (1997) reported that the value of  $\chi_{ARM}/\chi$  depends on the concentration of magnetic minerals (ferromagnetic susceptibility). If the concentration of magnetite is low in the sediments, the intensity of interaction between magnetic grains decreases, thus the value of  $\chi_{ARM}$  becomes high (Sugiura, 1979). The reason for relatively high  $\chi_{ARM}/\chi$  values at sites PS5, PS6, and PS7 may be contribution of SD magnetite or the change of interaction between the magnetic grains.

### 5.2 Change in magnetic grains with burial depth

The downcore changes in rock magnetic parameters and geochemistry of the interstitial water are shown in Fig. 9. The DO in the interstitial waters decreases with burial

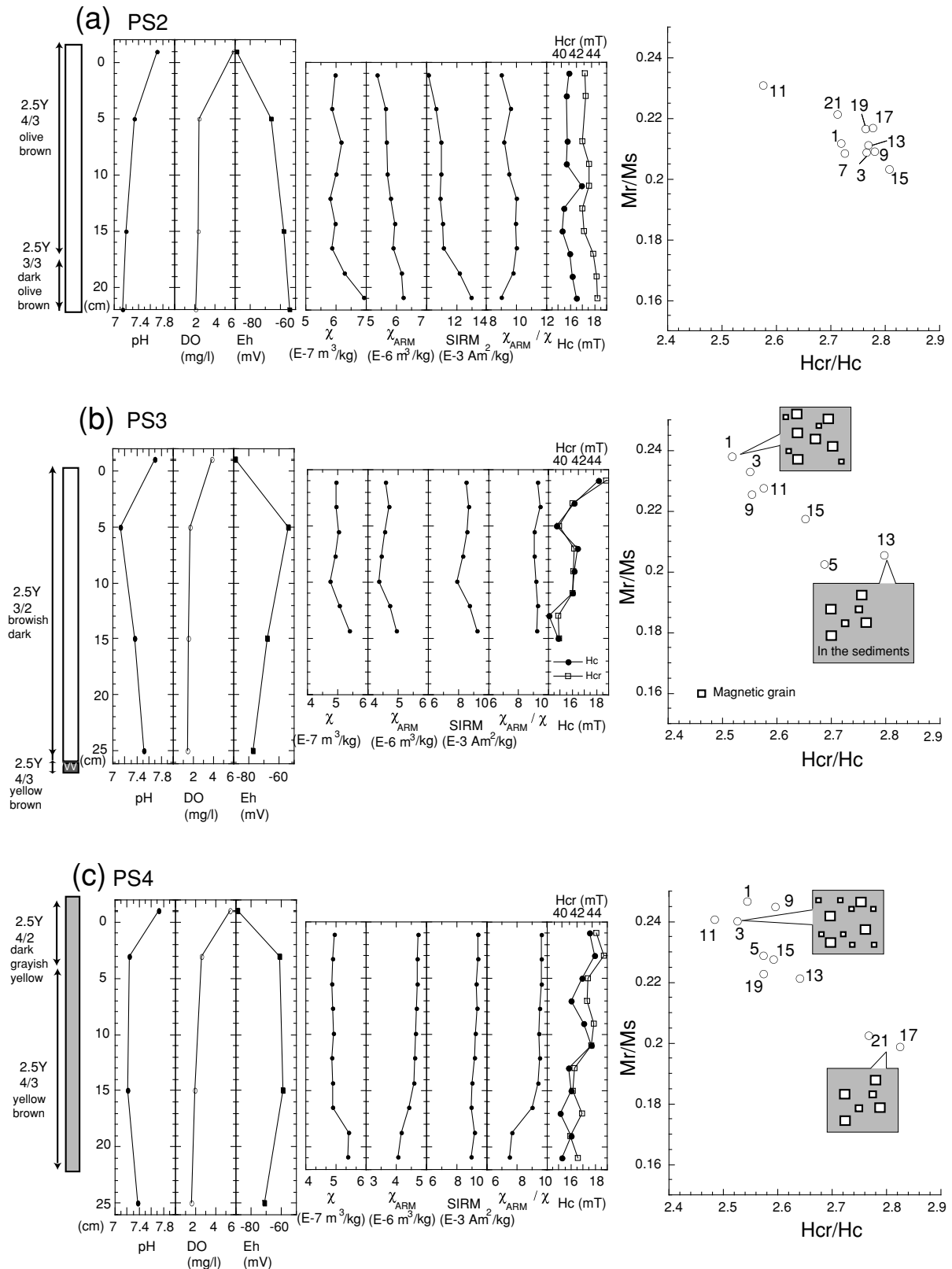


Fig. 9. Lithology, interstitial water pH, DO, and Eh values vs. depth,  $\chi$ ,  $\chi_{\text{ARM}}$ ,  $\text{SIRM}$ ,  $H_{\text{cr}}$ ,  $H_{\text{c}}$ , and hysteresis ratios for cores PS2, PS3 and PS4. The numbers in the Day plot indicate the sample depth within each core. Grey boxes show conceptual models for magnetic grain size (open square) distributions in the samples.

depth. The Eh increases with depth in core PS2, while it increases immediately below the surface, then decreases with depth in cores PS3 and PS4. The pH decreases with depth in core PS2, but it increases below 3–5 cmbsf in cores PS3 and

PS4. These results suggest that these sediments are under an anoxic condition with increasing burial depth and that the sediments at site PS2 is more oxic than these at sites PS3 and PS4.

The amount of magnetic mineral does not change significantly with burial depth. According to the Eh-pH diagram presented by Piper (1987), when pH or Eh decreases, magnetite is decomposed, ferrous iron is precipitated, and pyrite is formed. Magnetic mineralogy does not change with burial depth (Figs. 3 and 4) and, consequently, authigenic magnetic minerals are not formed and the maghemite rim of magnetite is not dissolved. However, the magnetic grain size, as estimated by the  $Mrs/Mr$  and  $Hcr/Hc$  ratios, changes in accordance with the geochemical changes in the interstitial water. Particularly for cores PS3 and PS4, the data points move to the lower right corner in the Day plots from 5 to 15 cmbsf, where the pH and Eh decrease. At 5 cmbsf in core PS3,  $Hcr$  and  $Hc$  decrease at the same horizon as the Eh peak and pH drop. Kawamura and Kawamura (2006) reported that these cores show no significant change in lithology. Considering the correspondence of the magnetic grain-size change to the geochemistry of the interstitial water, the changes in hysteresis parameters in these three cores might be due to dissolution of fine-grained magnetite as the result of early diagenesis (e.g., Tarduno and Wilkinson, 1996).

A model of dissolution of fine-grained magnetite is presented in Fig. 9 on the Day plots. In cores PS3 and PS4, fine-grained magnetite was dissolved, and the average grain size increases with burial depth. No significant differences were observed in the TOC values for the three cores (Fig. 6(c)), and the seawater temperatures around the coring sites are stable (Hase and Minato, 2003). The DO value of the seawater is the highest at site PS2 and remains above 2 mg/l with burial depth. On the other hand, the DO is relatively low and the Eh decreases with depth in cores PS3 and PS4. This suggests that the sediments shift to an anoxic condition in cores PS3 and PS4, accompanied by the dissolution of fine-grained magnetite.

## 6. Conclusions

Seven cores were collected from the Ryukyu Trench. The results of analyses on the magnetic properties and the geochemistry of the sediments have led the following conclusions.

1. Bottom water conditions at the landward slope, trench floor, and seaward slope are relatively suboxic, anoxic, and oxic, respectively, in the Ryukyu Trench. The grain sizes of the core sediments become gradually finer with increasing distance from the Okinawa Island, and finer with increasing water depth. The organic matter in the sediments is of marine origin.
2. The magnetic carriers within the sediments from the Ryukyu Trench are dominantly magnetite, maghemitized magnetite, and a minor amount of hematite.
3. The observed  $\chi$ ,  $\chi_{ARM}$ , and SIRM values indicate that the concentration of magnetic minerals is higher in the seaward cores than in the landward slope cores. This can be explained by a large supply of microfossils at the landward slope sites, which dilutes the concentration of magnetic minerals.
4. The granulometric parameters,  $\chi_{ARM}/\chi$  and  $SIRM/\chi$ , display slightly higher values in the landward slope sediments. This apparently suggests that the grain size of the magnetite is relatively finer at these cores. However, the hysteresis data from these cores suggests coarser magnetic grains. The results of high-temperature magnetometry indicate the presence of hematite. The reason for relatively high value of  $\chi_{ARM}/\chi$  may be due to the presence of fine-grained magnetite or the change of interaction between magnetic grains, and the reason of high  $SIRM/\chi$  may be a higher proportion of hematite in the samples.
5. The downcore change of the magnetic mineral assemblage in homogeneous sediments was caused by the dissolution of fine-grained magnetite during early diagenesis. The pattern of dissolution of fine-grained magnetite is different among the three cores and correlates with the redox condition in the interstitial water. Our results suggest that the fine-grained magnetite is susceptible to dissolution under an anoxic condition.

**Acknowledgments.** We thank Profs. Masayuki Torii and Akira Hayashida for their assistance in the magnetic measurements. We also thank Prof. Masahito Sugiyama for the geochemical measurements, and Dr. Ken Ikehara for the grain-size measurements. We are also deeply grateful to Prof. Suguru Ohta, the shipboard scientists, the captain and his crew of the KH05-1 cruise. Critical comments from Dr. Toshitsugu Yamazaki, Dr. Stefanie A. Branchfeld, and an anonymous reviewer have also been invaluable. A part of the study was supported by a Grant-in-Aid for young researchers from the Fukada Geological Institute (No. 15) and Paleo Labo Co., Ltd.

## References

- Banerjee, S. K., C. P. Hunt, and X.-M. Liu, Separation of local signals from the regional paleomonsoon record of the Chinese loess plateau: A rock-magnetic approach, *Geophys. Res. Lett.*, **20**(9), 843–846, 1993.
- Berner, R. A., *Early diagenesis: A theoretical approach*, 241 pp., Princeton University Press, Princeton, 1980.
- Bloemendal, J., J. W. King, F. R. Hall, and S.-J. Doh, Rock magnetism of Late Neogene and Pleistocene deep-sea sediments: relationship to sediments source, diagenetic processes and sediment lithology, *J. Geophys. Res.*, **97**, 4361–4375, 1992.
- Carman, R. and L. Rahm, Early diagenesis and chemical characteristics of interstitial water and sediments in the deep deposition bottoms of the Baltic proper, *J. Sea Res.*, **37**, 25–47, 1997.
- Day, R., M. Fuller, and V. A. Schmidt, Hysteresis properties of titanomagnetites: grain-size and compositional dependence, *Phys. Earth Planet. Inter.*, **13**, 260–267, 1977.
- Dunlop, D. J., Theory and application of the Day plot ( $Mrs/Ms$  versus  $Hcr/Hc$ ) II. Application to data for rocks, sediments, and soils, *J. Geophys. Res.*, **105**(B3), 10.1029/2001JB000487, 2002.
- Dunlop, D. J. and Ö. Özdemir, *Rock magnetism—Fundamentals and frontiers—*, 573 pp., Cambridge University Press, UK, 1997.
- Emerson, S. and J. I. Hedges, Processes controlling the organic carbon content of open ocean sediments, *Paleoceanography*, **3**, 621–634, 1988.
- Evans, M. E. and F. Heller, *Environmental Magnetism, Principles and applications of enviromagnetics*, 299 pp., Elsevier Science, USA, 2003.
- Froelich, P. N., G. P. Klinkhammer, M. L. Bender, N. A. Luedtke, G. R. Feath, D. Cullen, P. Daphin, D. Hammond, B. Hartman, and V. Maynard, Early oxidation of organic matter in pelagic sediments of the eastern equatorial Atlantic: suboxic diagenesis, *Geochim. Cosmochim. Acta*, **34**, 1075–1090, 1979.
- Garming, J. F. L., U. Bleil, and N. Riedinger, Alteration of magnetic mineralogy at the sulfate methane transition: Analysis of sediments from the Argentine continental slope, *Phys. Earth Planet. Inter.*, **151**, 290–308, 2005.
- Hase, H. and S. Minato, *R/V Mirai Cruise Report MR03-K03 (Leg 1 and Leg 2) June 7–July 30*, 141 pp., Japan Marine Science and Technology Center, Japan, 2003.

- Hirt, A. M., L. Lanci, J. Dobson, P. Weidler, and A. U. Gehring, Low-temperature magnetic properties of lepidocrocite, *J. Geophys. Res.*, **107**(B1), 2011, 2002.
- Ishikawa, N. and G. M. Frost, Magnetic properties of sediments from Ocean Drilling Program sites 1109, 1115 and 1118 (Leg 180), Woodlark Basin (Papua New Guinea), *Earth Planets Space*, **54**, 883–897, 2002.
- Karlin, R. and S. Levi, Diagenesis of magnetic minerals in recent hemipelagic sediments, *Nature*, **202**, 327–330, 1983.
- Kawamura, K. and N. Kawamura, Evolution of clay microstructures of superficial deep-Sea muds during burial compaction: examples from the Ryukyu Trench, *Geomechanics Geotechnics Particulate Media*, 3–8, 2006.
- Kawamura, N. and N. Ishikawa, Sedimentary environments in the Okinawa Trough and the Ryukyu Trench: evidence from paleomagnetic, rock magnetic, and geochemical analyses, *Rept. for Grant-in-Aid from Fukuda Geological Institute*, 116–121, 2006.
- Kawamura, N., H. Oda, K. Ikehara, T. Yamazaki, K. Shioi, S. Taga, S. Hatakeyama, and M. Torii, Diagenetic effect on magnetic properties of marine core sediments from the southern Okhotsk Sea, *Earth Planets Space*, **59**, 83–93, 2007.
- King, J. W., S. K. Banerjee, J. Marvin, and O. Ozdemir, A comparison of different magnetic methods for determining the relative grain size of magnetite in natural material: some results from lake sediments, *Earth Planet. Sci. Lett.*, **59**, 404–419, 1982.
- Kissel, C., C. Laj, A. Mazaud, and T. Dokken, Magnetic anisotropy and environmental changes in two sedimentary cores from the Norwegian Sea and the North Atlantic, *Earth Planet. Sci. Lett.*, **164**, 617–626, 1998.
- Leslie, B. W., D. E. Hammond, W. M. Berelson, and S. P. Lund, Diagenesis in anoxic sediments from the California continental borderland and its influence on iron, sulfur, and magnetite behavior, *J. Geophys. Res.*, **95**(B4), 4453–4470, 1990a.
- Leslie, B. W., S. P. Lund, and D. E. Hammond, Rock magnetic evidence for the dissolution and authigenic growth of magnetic minerals within anoxic marine sediments of the California continental borderland, *J. Geophys. Res.*, **95**, 4437–4452, 1990b.
- Liu, J., R. Zhu, A. P. Roberts, S. Li, and J.-H. Chang, High-resolution analysis of early diagenetic effects on magnetic minerals in post-middle-Holocene continental sediments from the Korea Strait, *J. Geophys. Res.*, **109**, 10.1029JB002813, 2004.
- Liu, Q., Y. Yu, J. Torrent, A. P. Roberts, Y. Pan, and R. Zhu, Characteristic low-temperature magnetic properties of aluminous goethite [ $\alpha$ -(Fe, Al)OOH] explained, *J. Geophys. Res.*, **111**(B12), 10.1029JB004560, 2006.
- Lowrie, W., Identification of ferromagnetic minerals in a rock by coercivity and unblocking temperature properties, *Geophys. Res. Lett.*, **17**, 159–162, 1990.
- Machida, H. and F. Arai, *Atlas of Volcanic Ash*, 276 pp., Tokyo University Press, Tokyo, Japan, 2003 (in Japanese).
- Maher, B. A., Magnetic properties of some synthetic sub-micron magnetites, *Geophys. J. R. Astron. Soc.*, **94**, 83–96, 1988.
- Moskowitz, B. M., R. B. Frankel, and D. A. Bazylinski, Rock magnetic criteria for the detection of biogenic magnetite, *Earth Planet. Sci. Lett.*, **120**, 283–300, 1993.
- Özdemir, Ö., D. J. Dunlop, and B. M. Moskowitz, The effect of oxidation on the Verwey transition in magnetite, *Geophys. Res. Lett.*, **20**(16), 1671–1674, 1993.
- Passier, H. F., M. J. Dekkers, and G. J. de Lange, Sediment chemistry and magnetic properties in an anomalously reducing core from the eastern Mediterranean Sea, *Chem. Geol.*, **152**, 287–306, 1998.
- Piper, J. D. A., *Palaeomagnetism and the Continental Crust*, 434 pp., Open University Press, Milton Keynes, UK, 1987.
- Rey, D., K. J. Mohamed, A. Bernabeu, B. Rubio, and F. Vilas, Early diagenesis of magnetic minerals in marine transitional environments: geochemical signatures of hydrodynamic forcing, *Mar. Geol.*, **215**, 215–236, 2005.
- Robinson, S. G., J. T. S. Sahota, and F. Oldfield, Early diagenesis in North Atlantic abyssal plain sediments characterized by rock-magnetic and geochemical indices, *Mar. Geol.*, **163**, 77–107, 2000.
- Stoner, J. S., J. E. T. Channell, and C. Hillaire-Marcel, Magnetic properties of deep-sea sediments off southwest Greenland: evidence for major differences between the last two deglaciations, *Geology*, **23**, 241–244, 1995.
- Sugiura, N., ARM, TRM and magnetic interactions: Concentration dependence, *Earth Planet. Sci. Lett.*, **42**, 451–455, 1979.
- Tarduno, J. A. and S. Wilkinson, Non-steady state magnetic mineral reduction, chemical lock-in, and delayed remanence acquisition in pelagic sediments, *Earth Planet. Sci. Lett.*, **144**, 315–326–84, 1996.
- Thompson, R. and F. Oldfield, *Environmental magnetism*, 227 pp., Allen & Unwin (Publishers) Ltd., London, UK, 1986.
- Torii, M., Low-temperature oxidation and subsequent downcore dissolution of magnetite in deep-sea sediments, ODP Leg 161 (Western Mediterranean), *J. Geomag. Geoelectr.*, **49**, 1223–1245, 1997.
- Ujiié, H. and Y. Ujiié, Late Quaternary course changes of the Kuroshio current in the Ryukyu Arc region, northwestern Pacific Ocean, *Mar. Micro.*, **37**, 23–40, 1999.
- Veywey, E. J. W., Electron conduction of magnetite (Fe<sub>3</sub>O<sub>4</sub>) and its transition point at low temperatures, *Nature*, **144**, 327–328, 1939.
- Walden, J., F. Oldfield, and J. Smith, *Environmental magnetic a practical guide*, *Quaternary Research Association*, 243 pp., Quaternary Research Association, London, 1999.
- Yamazaki, T. and N. Ioka, Cautionary note on magnetic grain-size estimation using the ratio of ARM to magnetic susceptibility, *Geophys. Res. Lett.*, **24**, 751–754, 1997.
- Yamazaki, T., A. L. Abdelaziz, and K. Ikehara, Rock-magnetic changes with reduction diagenesis in Japan Sea surface sediments and preservation of geomagnetic secular variation in inclination during the last 30,000 years, *Earth Planets Space*, **55**, 327–340, 2003.

---

N. Kawamura (e-mail: kawamura-noriko@aist.go.jp), K. Kawamura, and N. Ishikawa